Dominant density parameters and local pseudopotentials for simple metals

Carlos Fiolhais
Departamento de Física da Universidade de Coimbra, P-3000 Coimbra, Portugal

John P. Perdew, Sean Q. Armster, and James M. MacLaren
Department of Physics and Quantum Theory Group, Tulane University, New Orleans, Louisiana 70118

Marta Brajczewska
Departamento de Física da Universidade de Coimbra, P-3000 Coimbra, Portugal
(Received 20 January 1994; revised manuscript received 25 October 1994)

The properties of the simple metals are controlled largely by three density parameters: the equilibrium average valence electron density $3/4\pi r_s^3$, the valence z, and the density on the surface of the Wigner-Seitz cell, represented here by the equilibrium number $N_{\rm int}$ of valence electrons in the interstitial region. To demonstrate this fact, and as a refinement of the "stabilized jellium" or "structureless pseudopotential" model, we propose a structured local electron-ion pseudopotential $w(r)$ which depends upon either r_s and z ("universal" choice for $N_{\rm int}$), or r_s, z, and $N_{\rm int}$ for each metal ("individual" potential). Calculated binding energies, bulk moduli, and pressure derivatives of bulk moduli, evaluated in second-order perturbation theory, are in good agreement with experiment for 16 simple metals, and the bulk moduli are somewhat better than those calculated from first-principles nonlocal norm-conserving pseudopotentials. Structural energy differences agree with those from a nonlocal pseudopotential calculation for Na, Mg, and Al, but not for Ca and Sr. Our local pseudopotential $w(r)$ is analytic for all r, and displays an exponential decay of the core repulsion as $r \to \infty$. The decay length agrees with that of the highest atomic core orbital of s or p symmetry, corroborating the physical picture behind this "evanescent core" form. The Fourier transform or form factor $w(Q)$ is also analytic, and decays rapidly as $Q \to \infty$; its first and only zero Q_0 is close to conventional or empirical values. In comparison with nonlocal pseudopotentials, local ones have the advantages of computational simplicity, physical transparency, and suitability for tests of density functional approximations against more-exact many-body methods.

I. INTRODUCTION

The Hohenberg-Kohn theorem[1] tells us that the properties of a crystal are fixed by the electron density distribution $n(\mathbf{r})$ inside a unit cell, but does not tell us which if any features of the density dominate. For simple or sp-bonded metals in close-packed structures, the dominant density parameters are the equilibrium average valence electron density, represented by the density parameter r_s,

$$\overline{n} = 3/4\pi r_s^3 = k_F^3/3\pi^2 \ , \tag{1.1}$$

and the valence z. Together these parameters define the radius r_0 of the Wigner-Seitz sphere, whose volume is the volume per atom,

$$r_0 = z^{1/3} r_s \ . \tag{1.2}$$

A third parameter is the electron density averaged over the surface of the Wigner-Seitz sphere, which is correlated with the bulk modulus[2,3] and plays a role in Miedema's rule for the heat of formation of a binary alloy.[4] We shall work with a nearly equivalent parameter, the number $N_{\rm int}$ of valence electrons in the interstitial region between the polyhedral surface of the Wigner-Seitz cell of a monatomic crystal and the surface of the largest inscribed sphere.

In earlier work, we have developed a "stabilized jellium" or "structureless pseudopotential" model,[5] which achieves equilibrium at any chosen r_s (unlike jellium, which is stable only at $r_s = 4.1$ bohr). The only inputs to the model are r_s and z, and the outputs include realistic estimates of the bulk and surface properties of the simple metals, including void and cluster properties. Exceptions to this statement are the bulk modulus and its pressure derivative for the polyvalents, where the crystal structure plays an important role. In the present work, we will show that a *structured* pseudopotential model whose only inputs are r_s and z (our "universal" pseudopotential) corrects the worst errors of stabilized jellium, while an "individual" pseudopotential which also reproduces $N_{\rm int}$ is quantitatively accurate for all the simple metals. The extent to which this pseudopotential is transferable from the solid state to other environments will be the subject of a later study.

The goal of pseudopotential theory[6–8] is to obtain the key physical properties of atoms, molecules, and solids by dealing only with the valence electrons. To avoid a complicated all-electron problem, an effective weaker potential between the valence electrons and the atomic core is introduced. Interactions among the valence electrons are often described by density functional theory.[9]

Pseudopotentials which exactly match the valence elec-

tron orbital energies have been derived by orthogonality arguments,[10] and those which reproduce the valence electron orbitals outside the core have been derived by norm-conserving methods.[11] Those constructions typically start from the free atom, leaving open the question of transferability to the solid state. Moreover, they produce *nonlocal* pseudopotentials $w(\mathbf{r},\mathbf{r}')$, although some success has been achieved with semiempirical local pseudopotentials $w(\mathbf{r})$.

A local pseudopotential $w(\mathbf{r})$ can match the electron density $n(\mathbf{r})$ outside the cores, but a nonlocal one $w(\mathbf{r},\mathbf{r}')$ would be needed to match the Kohn-Sham density matrix $\rho(\mathbf{r},\mathbf{r}')$ in this region. If the properties of the simple metals are set by just a few density parameters, as we propose, then a *local* pseudopotential $w(\mathbf{r})$ which reproduces those dominant density parameters is fully justified. While the first goal of our study is to establish the idea of dominant density parameters, the second is to develop a comprehensive collection of accurate local pseudopotentials for the simple metals, using no empirical input except r_s. (z and $N_{\rm int}$ are theoretical inputs from an all-electron calculation.)

Nonlocal pseudopotentials are to be preferred for accurate predictions of the properties of real materials, and the use of nonlocal potentials is not a serious hindrance in most pseudopotential calculations. Nevertheless, local pseudopotentials have some advantages over nonlocal. (1) Their relative simplicity is an aid to conceptual understanding. (2) They are more convenient, and present practical advantages in complex calculations such as quantum Monte Carlo,[12,13] or in extensive studies of cohesion involving very many structures[14] or materials. (3) The Kohn-Sham scheme[15] of density functional theory requires that the external potential be *local*.[1,9,15] When it is nonlocal, the exchange-correlation energy is a functional of the noninteracting density matrix $\rho(\mathbf{r},\mathbf{r}')$,[16] and not just of the density $n(\mathbf{r})$.

For comparison of density functional pseudopotential approximations against experiment, point (3) is only a quibble. But this point is more germane to the testing of density functionals against the results of accurate quantum Monte Carlo calculations for solids or atoms. The Monte Carlo and density functional calculations typically invoke the same nonlocal pseudopotential; we suggest that our local pseudopotential would better meet the strict requirements of such a comparison.

The local pseudopotentials we propose here are constructed directly in and for the solid state, and to be used with the local density approximation (LDA).[15] Because these pseudopotentials reproduce the observed r_s by construction, they avoid the underestimation of r_s (by several percent) that LDA makes in first-principles all-electron or nonlocal pseudopotential calculations. Partly for this reason, the equilibrium properties of bulk simple metals are given somewhat more accurately by our local individual pseudopotential than by first-principles nonlocal norm-conserving pseudopotentials[17–21] (Table I). The root-mean-square relative errors for the bulk moduli of the metals in Table I are 12% for our local pseudopotentials, 18% for the nonlocal ones, and 13% for the all-electron calculations of Ref. 2.

TABLE I. Comparison of bulk properties for some simple metals calculated with norm-conserving (NC) nonlocal pseudopotentials and with our individual (I) local pseudopotentials against experiment (X). r_s is the density parameter of Eq. (1.1) in bohr, while B in Mbar and B' are the bulk modulus and its pressure derivative.

Metal	Method	r_s	B	B'
Be	NC[a]	1.85	1.310	–
	I	1.87	0.867	3.8
	X	1.87	1.144	4.6
Al	NC[b]	2.05	0.715	–
	I	2.07	0.771	4.4
	X	2.07	0.794	4.7
Mg	NC[c]	2.55	0.418	–
	I	2.65	0.314	4.2
	X	2.65	0.369	3.9
Li	NC[d]	3.17	0.130	2.6
	I	3.24	0.140	3.6
	X	3.24	0.133	3.5
Na	NC[d]	3.76	0.096	4.1
	I	3.93	0.071	3.6
	X	3.93	0.073	3.9
K	NC[d]	4.75	0.043	3.8
	I	4.86	0.034	3.7
	X	4.86	0.037	4.1
Rb	NC[e]	5.03	0.035	3.9
	I	5.20	0.026	3.6
	X	5.20	0.029	4.1

[a]Reference 17.
[b]Reference 18.
[c]Reference 19.
[d]Reference 20.
[e]Reference 21.

The *sp*-bonded metals are "simple" and deserve an accurate theory which is comparably simple. The extent to which these ideas can be extended to other classes of materials will be explored in a later study.

Our pseudopotentials have been tested for 16 simple metals, in the framework of second-order perturbation theory and using local-field exchange-correlation corrections to the Lindhard dielectric function. In particular, we have evaluated binding energies e, bulk moduli B, and pressure derivatives of bulk moduli $B' = dB/dP$, and compared them with experimental values. Chemical potentials μ have also been calculated, as have structural energy differences. Omitted from our list of simple metals are the noble metals Cu, Ag, and Au, and their neighbors in the periodic table, Zn, Cd, and Hg, which may show significant core-electron contributions to cohesion. Ga, In, and Tl, which are less suspect, have been included.

In the conventional view, at best eight of these metals (Na, K, Rb, Cs, Mg, Al, Ga, and In) have reasonably local pseudopotentials which can be treated accurately by nonrelativistic second-order perturbation theory. However, our calculations for the perfect crystals at or near their equilibrium volumes present little evidence (except in the structural energy differences for Ca, Sr, and Ba) for nonlocality or for the inadequacy of nonrelativistic

perturbation theory in any of the 16 simple metals. The need for nonlocality will show itself more clearly when we attempt to transfer those local pseudopotentials to radically different environments, such as the free atom.[22]

The outline of this paper is as follows. Section II reviews some previous work which is related to our own, presents our new evanescent core form for the local pseudopotential, and discusses how to fix its two parameters. In Sec. III, we show the results for e, B, B', μ, and the structural energy differences, based upon the universal and individual versions of this potential, and show that one of the two parameters has a transparent physical interpretation. Section IV summarizes our conclusions.

A brief announcement of this work, with preliminary values for $N_{\rm int}$, appears in Ref. 23.

II. THE EVANESCENT CORE POTENTIAL

Before introducing our new pseudopotential, we shall review some related work with local pseudopotentials.

The Ashcroft electron-ion pseudopotential is local and characterized by a single parameter r_c, the radius of the empty core,

$$w^A(r) = -\frac{z}{r}\theta(r - r_c) \ , \tag{2.1}$$

with z the valence and $\theta(x)$ the step function. (We use hartree atomic units $\hbar = m = e^2 = 1$.) The value of r_c may be taken from Fermi surface data or measured transport properties of solids, which are sensitive to the first zero of the form factor. In practice, the simple form (2.1) is inadequate for an accurate calculation of bulk properties of the simple metals (atomic volume, binding energy, and bulk modulus). It is clear from Table 2 of Ref. 24 that "Ashcroft pseudopotentials with unadjusted zeroth Fourier component ... lead to disaster for any reasonable choice of r_c," when used to calculate the bulk modulus by the method of homogeneous deformation. To surmount this problem, Ashcroft and Langreth,[25] in a second-order perturbative calculation, decoupled the zeroth Fourier coefficient of this potential, which they determined instead from the equilibrium condition of zero pressure at the observed average electron density. Moreover, they retained only the first shell of reciprocal lattice vectors. Thus they modified both the average value and the short-range behavior of the potential (2.1) in such a way that the result cannot be transferred from the bulk solid to other arrangements of atoms. However, they did identify the important physics and so found realistic results for the binding energy and bulk modulus of the simple metals, including the polyvalents for which the band-structure contribution to the bulk modulus is crucial.

The Ashcroft potential may be viewed as a special case of a family of pseudopotentials (the so-called Heine-Abarenkov pseudopotentials[26]) characterized by a constant value, not necessarily zero, of the potential inside the core. These two-parameter pseudopotentials are

$$w^{\rm HA}(r) = \begin{cases} zu/R, & r \le R \\ -z/r, & r > R, \end{cases} \tag{2.2}$$

with u a constant. Shaw[27] has presented the case for the continuous potential obtained with $u = -1$: its quicker convergence in reciprocal space is a clear advantage. Ling and Gelatt[28] have used the Shaw potential to account for the bulk and shear moduli of simple metals. Unlike Ashcroft and Langreth, Ling and Gelatt did not use any empirical input besides the average density and the valence; we call a potential constructed in that way a universal pseudopotential. Stabilization of the metal at the observed density was used to determine R. A sum over relevant reciprocal lattice vectors was performed. Like Ashcroft and Langreth, Ling and Gelatt neglected the local-field exchange-correlation contribution to the band-structure energy. Unfortunately, as noted in Ref. 28, the Ling-Gelatt potential has unphysical values for the first zero of its form factor.

In the present work, we propose a local pseudopotential which, in contrast to the Shaw form, is not only continuous but has continuous derivatives. We were motivated to search for such a smooth local pseudopotential by two main considerations. (1) Smoothness leads to a better convergence of sums over reciprocal lattice vectors. (2) Smoothness and evanescence (exponential decay of the core repulsion as $r \to \infty$) are properties to be expected from the orthogonalization construction[10] of a pseudopotential. The first pseudopotential, proposed by Hellmann[29] in 1934, had an evanescent form, but this was lost in the rediscovery of pseudopotentials which occurred in the 1960s. [See, however, Refs. 6 (Sec. 8.8), 30, 31, and 32.]

At $r = 0$, our potential is designed to have a finite value and vanishing first and third derivatives. This analyticity guarantees a quick convergence of its Fourier transform $\lim_{Q\to\infty} w(Q) \sim Q^{-8}$, in contrast with the Shaw potential, which goes only like Q^{-3} for large Q. At large r, our potential approaches the Coulomb tail, with a contribution from the core which decays exponentially (like a core orbital).

This evanescent core pseudopotential may be written as

$$w(r) = -\frac{z}{R}\left\{\frac{1}{x}[1 - (1 + \beta x)e^{-\alpha x}] - Ae^{-x}\right\} \ , \tag{2.3}$$

with $x = r/R$, R being a core decay length, and with $\alpha > 0$. An analyticity condition at $r = 0$ determines A and β in terms of α. However, if we choose instead to treat all four parameters as independent, then Eq. (2.3) reduces to the form used by Krasko and Gurskii[32] when $\beta = 0$ and $\alpha = 1$, and to the form used by Harrison in Sec. 8.8 of Ref. 6 when β is finite and $\alpha \to \infty$. Equation (2.3) is not broad enough to encompass the form used in Refs. 29 and 30, which represents the repulsion by $Ce^{-r/R}/r$, except when $C = z$, or that used in Ref. 31, which cannot be Fourier transformed analytically.

The pseudopotential concept may be justified by the construction of Austin, Heine, and Sham,[10] in which the pseudopotential is written as

$$w = V + \sum_c A_c |\psi_c\rangle\langle\psi_c| \ , \tag{2.4}$$

where V is the real potential, the A_c are constants (real numbers), and the $|\psi_c\rangle$ are core states. In the limit $r \to \infty$, the last term can be represented in real space by $Ae^{-r/R}$, with R a parameter which measures the decay length of the core, when (2.4) is applied to a wave function which does not vary significantly over the core. The core electron density decays as $e^{-2r/R}$.

The evanescent core pseudopotential (2.3), with $\alpha > 1$, has the right behavior at $x \to \infty$:

$$w \to -\frac{z}{r} + \frac{zA}{R} e^{-r/R} . \tag{2.5}$$

On the other hand, when $x \to 0$,

$$w \to -\frac{z}{R} \left\{ [\alpha - \beta - A] + x \left[-\frac{1}{2}\alpha^2 + \alpha\beta + A \right] + \frac{x^2}{2} \left[\frac{1}{3}\alpha^3 - \alpha^2\beta - A \right] + \frac{x^3}{6} \left[-\frac{1}{4}\alpha^4 + \alpha^3\beta + A \right] + \cdots \right\} . \tag{2.6}$$

We impose the following analyticity (cusp-free) conditions:

$$-\tfrac{1}{2}\alpha^2 + \alpha\beta + A = 0 , \tag{2.7}$$

$$-\tfrac{1}{4}\alpha^4 + \alpha^3\beta + A = 0 . \tag{2.8}$$

From these equations we obtain

$$\beta = \frac{\alpha^3 - 2\alpha}{4(\alpha^2 - 1)} , \tag{2.9}$$

$$A = \frac{1}{2}\alpha^2 - \alpha\beta . \tag{2.10}$$

We are therefore left with two parameters, α and R. The parameter A is positive for $\alpha > 1$. If $\alpha > 1 + \sqrt{3}$, then $w(r = 0) > 0$. If $R \to 0$ at fixed α, then $w(r) \to -z/r$. If $\alpha \to 0$ at fixed R, then $w(r)$ vanishes identically.

In Fourier space, the conditions (2.7) and (2.8) have a simple meaning: they make the potential fall off like Q^{-8}, since the contributions proportional to Q^{-4} and Q^{-6} vanish. In fact, the Fourier transform of $w(r)$ is

$$w(Q) = \int_0^\infty dr\ 4\pi r^2 w(r) \frac{\sin Qr}{Qr} = 4\pi z R^2 \left[-\frac{1}{(QR)^2} + \frac{1}{(QR)^2 + \alpha^2} + \frac{2\alpha\beta}{[(QR)^2 + \alpha^2]^2} + \frac{2A}{[(QR)^2 + 1]^2} \right] . \tag{2.11}$$

From Eqs. (2.9), (2.10), and (2.11) we find

$$\lim_{Q \to \infty} w(Q) = 4\pi z[-\alpha^6 + 6\alpha^5\beta + 6A]R^{-6}Q^{-8} . \tag{2.12}$$

In the other limit,

$$\lim_{Q \to 0} w(Q) = -\frac{4\pi z}{Q^2} + \frac{z}{\bar{n}} \overline{w}_R , \tag{2.13}$$

where the volume-averaged core repulsion

$$\overline{w}_R = 4\pi\bar{n}R^2 \left[\frac{1}{\alpha^2} + 2\left(\frac{\beta}{\alpha^3} + A \right) \right] \tag{2.14}$$

is positive for all $\alpha > 0$.

Straightforward algebra shows that the single zero Q_0 of $w(Q)$ is given by

$$(Q_0 R)^2 = \frac{2}{\alpha^2 - 3} . \tag{2.15}$$

In order to have a real zero, we need $\alpha > \sqrt{3}$.

For a given metal, the two parameters R and α are fixed by two conditions: The binding energy e should minimize at the observed density parameter r_s, as in Eq. (3.10), and the valence interstitial electron number $N_{\rm int}$ should equal either its uniform-electron-gas value (universal pseudopotential fixed by r_s and z) or its actual value for each metal (individual pseudopotential fixed by r_s, z, and $N_{\rm int}$). The actual value of $N_{\rm int}$ is found from the valence electron density of an all-electron calculation at the observed bulk density within the local density approximation,[15,33] using a full-potential version of a linearized augmented Slater-type orbital (LASTO) program.[34] The STO basis functions for the interstitial region included two s-type, six p-type, ten d-type, and seven f-type functions (i.e., s, p, and d functions for two principal quantum numbers, and an f function for one principal quantum number). In an attempt to smuggle some relativistic effects into a nonrelativistic pseudopotential, the LASTO calculations were performed at the scalar-relativistic level, using the approach of Koelling and Harmon.[35] For the fcc (bcc) structures, 110 (70) special k points[36] in the irreducible wedge of the Brillouin zone were used, and 283 (249) reciprocal lattice vectors were retained in the Fourier expansion of each orbital in the interstitial region; for the hcp crystal, 72 special k points and 311 plane waves were used. Within each sphere, the wave function was truncated at $l = 6$, while the potential was truncated at $l = 8$.

To fit $N_{\rm int}$, only the bcc, fcc, and hcp structures were used; tetragonal and orthorhombic metals were treated as fcc. (Only bcc and fcc structures were used to calculate $N_{\rm int}$ in Ref. 2.) In terms of the radius r_0 of the Wigner-Seitz sphere, the radius $r_{\rm min}$ of the inscribed (or muffin-tin) sphere is $0.879\,44 r_0$ (bcc), $0.904\,70 r_0$ (fcc), and $f(c/a)r_0$ (hcp), where

$$f(x) = \begin{cases} 1.065\,37\ x^{-1/3}, & x > \sqrt{\frac{8}{3}} \\ 1.065\,37 x^{-1/3} \left[\frac{1}{3} + \frac{1}{4}x^2 \right]^{1/2}, & x < \sqrt{\frac{8}{3}} \end{cases} .$$

Then the uniform-gas value of $N_{\rm int}$ is

$$N_{\rm int}^{\rm unif} = z\left[1 - \left(\frac{r_{\rm min}}{r_0} \right)^3 \right] . \tag{2.16}$$

The result of first-order perturbation theory is

$$N_{\rm int} = N_{\rm int}^{\rm unif} - 4\pi \frac{\overline{n}}{z} \sum_{\mathbf{G} \neq \mathbf{0}} \frac{w(G)[\mathrm{Re}\ s(\mathbf{G})]\chi(G)}{\epsilon(G)G^3} \times \left[\sin x - x\cos x \right] \Big|_{x = G r_{\rm min}} , \tag{2.17}$$

where $\mathbf{G}$ denotes a reciprocal lattice vector, and

$$s(\mathbf{G}) = \frac{1}{p}\sum_{\alpha=1}^{p} \exp(-i\mathbf{G}\cdot\mathbf{d}_\alpha) \tag{2.18}$$

is the structure factor for the basis of p atoms in the primitive unit cell, which reduces to unity for $p = 1$. Equation (2.17) is derived by subtracting the number of electrons in a sphere of radius $r_{\min}$ from the number z in the Wigner-Seitz cell. $\chi(G)$ and the dielectric function $\epsilon(G)$ are defined in Eqs. (3.6) and (3.7).

III. RESULTS

The binding energy per electron of a homogeneous electron gas in the field of a positive charge background (jellium model) is

$$e^J(\overline{n}) = \frac{3k_F^2}{10} - \frac{3k_F}{4\pi} + e_c(\overline{n}) \ , \tag{3.1}$$

where the first term is the kinetic energy, the second the exchange energy, and the third the correlation energy.[33]

The electrostatic energy of the jellium model is zero. This description of the valence electrons of a metal can be significantly improved by taking into account, in first-order perturbation theory, the localized ions of a real lattice. Then, the energy incorporates a Coulomb part, due to the attraction between the electronic density and the positive charges and the self-repulsion of both the electronic cloud and the positive background, and a non-Coulomb contribution due to the repulsion of the valence electrons from the core, as described by a pseudopotential.

To first order, the total binding energy (energy to assemble the valence electrons and ions to form the solid) is

$$e^{\mathrm{SJ}} = e^J + e_M + \overline{w}_R \ , \tag{3.2}$$

with

$$e_M \simeq -\frac{9z^{2/3}}{10r_s} \tag{3.3}$$

the Madelung energy (electrostatic energy of point ions in a uniform negative background) and $\overline{w}_R$ the average repulsive part of the pseudopotential, which is given by Eq. (2.14) for the evanescent core potential. (We have used the exact Madelung energy[37] for each bcc, fcc, or nonideal hcp lattice in our calculations.) From the stability condition

$$\frac{\partial}{\partial r_s} e^{\mathrm{SJ}}(r_s, z, \overline{w}_R) = 0, \tag{3.4}$$

the stabilized jellium (SJ) value of $\overline{w}_R$ is determined. The model defined by (3.2) and (3.4) is "bulk stabilized jellium."[5] In this simplified model, the value of $\overline{w}_R$ does not depend upon the form of the local pseudopotential.

We have not yet taken into account the inhomogeneity of the electron gas in a real solid. For that purpose, we use second-order perturbation theory.[25,38,39] The band-structure energy which must be added to (3.2) is

$$e_{\mathrm{BS}} = \frac{1}{2}\sum_{\mathbf{G}\neq\mathbf{0}} \left(\frac{\overline{n}_i}{\overline{n}}\right)^2 |w(G)s(\mathbf{G})|^2 \frac{\chi(G)}{\epsilon(G)}\overline{n} \ , \tag{3.5}$$

where $\overline{n}_i$ denotes the average ion density ($\overline{n}/\overline{n}_i = z$ for a neutral system),

$$\chi(G) = -\frac{k_F}{\pi^2} F(y) \ ,$$
$$F(y) = \frac{1}{2} + \frac{1-y^2}{4y}\ln\frac{|1+y|}{|1-y|} \ , \quad y = \frac{G}{2k_F} \ , \tag{3.6}$$

and $\epsilon(G)$ is the Lindhard dielectric function

$$\epsilon(G) = 1 - 4\pi\frac{\chi(G)}{G^2}[1 - \mathcal{G}_{\mathbf{xc}}(G)] \ . \tag{3.7}$$

Here

$$\mathcal{G}_{\mathbf{xc}}(G) = \gamma\, y^2, \quad \gamma = 1 - \frac{k_F^2}{\pi}\frac{\partial^2}{\partial\overline{n}^2}(\overline{n}e_c) \tag{3.8}$$

is the local-field correction in the local density approximation.[15,33,38] All sums over reciprocal lattice vectors $\mathbf{G}$ have been fully converged.

The binding energy per valence electron of the solid is therefore

$$e = e^J + e_M + \overline{w}_R + e_{\mathrm{BS}} \ . \tag{3.9}$$

The equilibrium condition is now

$$\frac{\partial}{\partial r_s} e(r_s, z, \alpha, R) = 0 \ . \tag{3.10}$$

In the case of hcp metals, this variation has been performed for a fixed c/a (experimental value).

Table II shows the result for R arising from (3.10). Comparing this R with the Hartree-Fock decay length $R_{\mathrm{HF}} = 1/\sqrt{-2e_{\mathrm{HF}}}$, with e_{HF} the Hartree-Fock energy of the highest core orbital of s or p type,[40] we note the overall good agreement. The main discrepancies occur for Be and Li. These elements have no p core state, making their first-principles pseudopotentials highly nonlocal.

Table II also shows universal and individual values for the first zero Q_0 of the form factor, from Eq. (2.15). The "individual" $Q_0/2k_F$ values agree rather well with conventional (mainly empirical) values from Ref. 7, also displayed in Table II.

Figures 1 and 2 illustrate the evanescent core potential, in real and momentum space, respectively, for a selection of simple metals.

The bulk modulus or elastic stiffness is

$$B = -V\left(\frac{\partial P}{\partial V}\right)_N = \frac{1}{12\pi}\left(\frac{1}{r_s}\frac{\partial^2 e}{\partial r_s^2} - \frac{2}{r_s^2}\frac{\partial e}{\partial r_s}\right) \ , \tag{3.11}$$

with $P = -\left(\frac{\partial E}{\partial V}\right)_N = -\frac{1}{4\pi r_s^2}\frac{\partial e}{\partial r_s}$ the pressure. The pressure derivative of the bulk modulus is

$$B' = \frac{dB}{dP} = \frac{dB/dr_s}{dP/dr_s} = -\frac{dB/dr_s}{3B/r_s} \quad . \tag{3.12}$$

We note that, at equilibrium, B' relates the second and third derivatives of the binding energy

$$\frac{\partial^3 e}{\partial r_s^3} = \frac{3}{r_s}\left(1 - B'\right)\frac{\partial^2 e}{\partial r_s^2} \quad . \tag{3.13}$$

The chemical potential is defined as

$$\mu = \frac{\partial}{\partial \overline{n}}(\overline{n}e)\Big|_{\overline{n}_i} = e - \frac{r_s}{3}\frac{\partial e}{\partial r_s}\Big|_{\overline{n}_i} = \mu^J + \langle \delta v \rangle_{\rm WS} + \mu_{\rm BS} \ , \tag{3.14}$$

where the derivative is taken at constant ionic density $\overline{n}_i$, and

$$\langle \delta v \rangle_{\rm WS} = -\frac{3}{10}\frac{z^{\frac{2}{3}}}{r_s} + \overline{w}_R \tag{3.15}$$

is the average over the Wigner-Seitz cell of the discrete lattice perturbation $\delta v(\mathbf{r})$. This bulk chemical potential μ, a second parameter of Miedema's rule,[4] is the Fermi level measured from the vacuum level, neglecting the relaxation of the electron density in cells near the surface. The work function is $\Delta\phi - \mu$, where $\Delta\phi$ is the surface-relaxation dipole barrier.

Table III shows the output of our calculations of equilibrium binding energies, bulk moduli, pressure derivatives of the bulk moduli, and chemical potentials performed with the evanescent core pseudopotential. The derivatives (3.11), (3.12), and the third term on the right

TABLE II. Parameters of the evanescent core potential in the universal (U) and individual (I) forms. The parameters α and R are determined from r_s, z, and $N_{\rm int}$ for a given lattice structure. The structures employed for most of the metals are the physical ones. We have used the "nominal" fcc structure in all calculations for Ga, Sn, and In. Perhaps because we do not make the muffin-tin approximation, our values of $N_{\rm int}$ are significantly lower than those of Refs. 2 and 3 for Ga, In, Sr, and Ba. $R_{\rm HF}$ is the Hartree-Fock decay length of the highest s or p core orbital, from Ref. 40. $(Q_0/2k_F)^{\rm conv}$ is the conventional first zero of $w(Q)$, from Ref. 7. (Double-digit values are solid-state empirical. Single-digit values are read from a plot of the Animalu-Heine form factor.) The unit of r_s, R, and $R_{\rm HF}$ is the bohr.

Metal	r_s	z	Structure		$N_{\rm int}$	α	R	$R_{\rm HF}$	$Q_0/2k_F$	$(Q_0/2k_F)^{\rm conv}$
Be	1.87	2	hcp	U	0.577	4.542	0.197		0.83	
			c/a=1.567	I	0.563	4.552	0.192	0.33	0.85	0.7
Al	2.07	3	fcc	U	0.779	3.635	0.334		0.71	
				I	0.705	3.573	0.317	0.39	0.77	0.75
Ga	2.19	3	rhombic	U	0.779	3.542	0.365		0.72	
				I	0.559	3.256	0.319	0.33	0.92	0.85
Sn	2.22	4	tetragonal	U	1.038	3.376	0.443		0.64	
				I	0.696	3.056	0.388	0.35	0.84	0.83
Pb	2.30	4	fcc	U	1.038	3.337	0.466		0.64	
				I	0.638	2.912	0.406	0.37	0.89	0.90
In	2.41	3	tetragonal	U	0.779	3.401	0.423		0.72	
				I	0.593	3.133	0.388	0.38	0.88	0.90
Tl	2.48	3	hcp	U	0.824	3.362	0.439		0.72	
			c/a=1.599	I	0.560	2.897	0.405	0.39	0.97	0.9
Mg	2.65	2	hcp	U	0.526	3.502	0.382		0.84	
			c/a=1.625	I	0.529	3.508	0.383	0.47	0.84	0.78
Li	3.24	1	bcc	U	0.320	3.549	0.361		1.07	
				I	0.344	4.133	0.341	0.45	0.93	0.8
Ca	3.27	2	fcc	U	0.519	3.194	0.535		0.84	
				I	0.548	3.279	0.538	0.61	0.80	0.7
Sr	3.57	2	fcc	U	0.519	3.098	0.609		0.84	
				I	0.552	3.194	0.612	0.67	0.80	0.7
Ba	3.71	2	bcc	U	0.640	3.006	0.647		0.86	
				I	0.693	3.128	0.649	0.74	0.81	0.7
Na	3.93	1	bcc	U	0.320	3.075	0.528		1.08	
				I	0.341	3.517	0.492	0.57	0.96	0.98
K	4.86	1	bcc	U	0.320	2.807	0.745		1.09	
				I	0.356	3.349	0.679	0.72	0.92	0.93
Rb	5.20	1	bcc	U	0.320	2.748	0.824		1.09	
				I	0.354	3.228	0.755	0.79	0.93	0.94
Cs	5.62	1	bcc	U	0.320	2.692	0.920		1.09	
				I	0.358	3.170	0.843	0.86	0.93	1.0

of (3.14) have been evaluated numerically, and checked by varying the r_s mesh. For the sake of comparison, the values obtained with the stabilized jellium model [Eqs. (3.2) and (3.4)] are displayed. In the latter case, the derivatives were obtained analytically.

Tables II and III display some clear trends. The band-structure contributions $e_{\rm BS}$ and $\mu_{\rm BS}$ depend strongly upon the choice of model, but within a given model $e_{\rm BS} \approx \mu_{\rm BS}$. When $N_{\rm int}$ is increased, holding the bulk stable at the observed r_s, the quantities α, e, B, B', and μ all increase, with approximately equal increases in e and μ, while $e_{\rm BS}$ and $\mu_{\rm BS}$ decrease to more negative values, and Q_0 decreases. However, the cohesive properties e, B, B', and μ are not very sensitive to such changes in $N_{\rm int}$ or Q_0 over a plausible range. As Q_0 changes, there are compensating changes in the $G = 0$ and $G \neq 0$ Fourier components of $w(G)$. Thus a precise determination of Q_0 requires fitting not to the cohesive properties but to some property that has *no* contribution from $w(G = 0)$, such as the interstitial electron density of Eq. (2.17).

The root-mean-square relative errors of the bulk moduli in Table III are 90% for the stabilized jellium (SJ) model, 40% for the universal pseudopotential (U), and only 11% for the individual pseudopotential (I).

The individual option of the pseudopotential leads, in most cases, to good agreement with experiment. An exception is the binding energy of Pb, where a spin-orbit correction of about 2 eV may be invoked to restore the agreement.[41] The bulk moduli of the tetravalents Pb and Sn are properly described only by the individual pseudopotential, which takes into account that $N_{\rm int} \ll N_{\rm int}^{\rm unif}$ in these metals.

TABLE III. Bulk binding energy per electron e, bulk modulus B, pressure derivative of the bulk modulus B', and chemical potential μ for the universal (U) and individual (I) choices of the evanescent core potential. SJ labels the stabilized jellium result. X refers to experimental values: e was taken from Ref. 55; B and B' were taken from a compilation in Ref. 56, except that B of Ga, Sn, and Sr were taken from Ref. 37, B' of Be, Sn, Tl, and Mg from Ref. 57, B and B' of In from Ref. 58, B' of Ba from Ref. 59, and B and B' of Na, K, and Rb from Ref. 60. The "X" values for μ are semiempirical estimates from Ref. 61. The unit of binding energy and chemical potential is the eV, while the unit of B is the Mbar (1 hartree = 27.21 eV, 1 hartree/bohr^3 = 294.2 Mbar). The structures used are the physical ones from Table II, except for Ga, Sn, and In, which were treated as fcc. (We have verified that r_s, B, and B' are nearly the same for the fcc, bcc, and hcp structures, when the pseudopotential is held fixed, for all metals in this table. Whether this is also true for the orthorhombic structure of Ga is an open question.) For the hcp structures, c/a was held fixed while r_s was varied.

Metal		e	($e_{\rm BS}$)	B	B'	μ	($\mu_{\rm BS}$)
Be	SJ	-16.51		1.722	3.2	0.68	
	U	-16.03	(-1.31)	0.899	3.9	1.10	(-1.36)
	I	-16.18	(-1.21)	0.867	3.8	0.96	(-1.26)
	X	-15.45		1.144	4.6	0.8	
Al	SJ	-19.10		1.576	3.2	-0.21	
	U	-18.49	(-1.24)	0.952	4.5	0.47	(-1.18)
	I	-19.05	(-0.86)	0.771	4.4	-0.17	(-0.88)
	X	-18.88		0.794	4.7	-0.8	
Ga	SJ	-18.20		1.279	3.2	-0.59	
	U	-17.64	(-1.08)	0.790	4.5	0.03	(-1.01)
	I	-19.61	(-0.60)	0.497	3.9	-1.83	(-0.43)
	X	-20.03		0.565	–	-2.4	
Sn	SJ	-21.22		1.471	3.3	-0.68	
	U	-20.55	(-1.54)	1.001	4.6	0.17	(-1.36)
	I	-23.03	(-0.74)	0.518	4.3	-2.24	(-0.49)
	X	-24.08		0.480	6.0	-3.1	
Pb	SJ	-20.57		1.287	3.3	-0.88	
	U	-19.91	(-1.43)	0.900	4.6	-0.04	(-1.25)
	I	-22.91	(-0.83)	0.433	4.2	-2.77	(-0.38)
	X	-24.68		0.488	5.5	-3.7	
In	SJ	-16.76		0.896	3.2	-1.11	
	U	-16.26	(-0.85)	0.578	4.5	-0.55	(-0.78)
	I	-17.63	(-0.41)	0.380	4.2	-1.91	(-0.33)
	X	-18.40		0.418	4.8	-2.6	
Tl	SJ	-16.34		0.805	3.2	-1.24	
	U	-15.91	(-0.75)	0.511	4.5	-0.78	(-0.73)
	I	-17.86	(-0.50)	0.330	4.0	-2.50	(-0.24)
	X	-19.42		0.382	5.7	-3.4	
Mg	SJ	-12.39		0.487	3.2	-1.49	
	U	-12.14	(-0.40)	0.310	4.2	-1.25	(-0.41)
	I	-12.12	(-0.41)	0.314	4.2	-1.23	(-0.42)
	X	-12.11		0.369	3.9	-1.7	

Metal		e	($e_{\rm BS}$)	B	B'	μ	($\mu_{\rm BS}$)
Li	SJ	-7.45		0.155	3.2	-1.95	
	U	-7.39	(-0.10)	0.133	3.5	-1.90	(-0.10)
	I	-7.28	(-0.36)	0.140	3.6	-1.80	(-0.39)
	X	-6.97		0.133	3.5	-1.9	
Ca	SJ	-10.33		0.222	3.3	-1.96	
	U	-10.15	(-0.23)	0.156	4.2	-1.82	(-0.26)
	I	-10.04	(-0.33)	0.167	4.2	-1.71	(-0.38)
	X	-9.91		0.152	3.2	-1.6	
Sr	SJ	-9.56		0.160	3.3	-2.05	
	U	-9.41	(-0.18)	0.114	4.2	-1.93	(-0.21)
	I	-9.29	(-0.29)	0.124	4.3	-1.81	(-0.33)
	X	-9.21		0.116	3.5	-1.6	
Ba	SJ	-9.24		0.138	3.3	-2.08	
	U	-9.13	(-0.12)	0.095	4.3	-1.96	(-0.12)
	I	-8.98	(-0.24)	0.105	4.3	-1.79	(-0.21)
	X	-8.54		0.103	3.4	-1.3	
Na	SJ	-6.34		0.076	3.2	-2.10	
	U	-6.30	(-0.04)	0.068	3.5	-2.06	(-0.04)
	I	-6.23	(-0.15)	0.071	3.6	-2.00	(-0.16)
	X	-6.25		0.073	3.9	-2.0	
K	SJ	-5.28		0.035	3.3	-2.07	
	U	-5.25	(-0.02)	0.031	3.6	-2.04	(-0.02)
	I	-5.17	(-0.15)	0.034	3.7	-1.98	(-0.16)
	X	-5.27		0.037	4.1	-2.2	
Rb	SJ	-4.98		0.027	3.3	-2.04	
	U	-4.95	(-0.01)	0.025	3.7	-2.01	(-0.01)
	I	-4.88	(-0.11)	0.026	3.6	-1.95	(-0.12)
	X	-5.02		0.029	4.1	-2.1	
Cs	SJ	-4.65		0.020	3.3	-1.99	
	U	-4.62	(-0.01)	0.018	3.6	-1.96	(-0.01)
	I	-4.56	(-0.11)	0.020	3.7	-1.90	(-0.11)
	X	-4.68		0.023	4.0	-2.2	

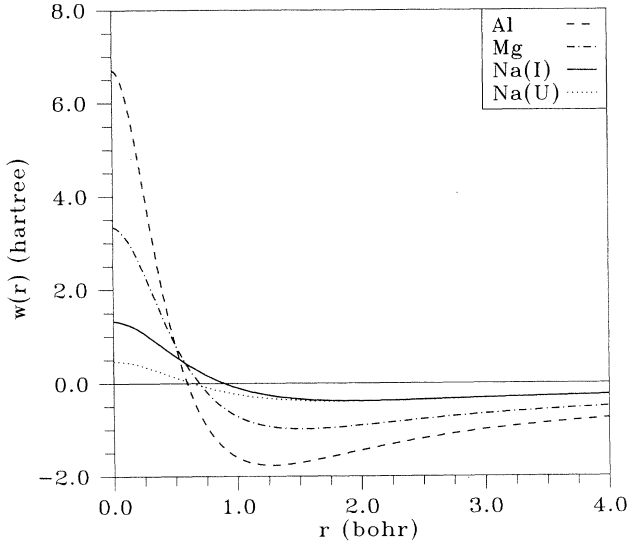

FIG. 1. Evanescent core potential in real space for Al and Mg (individual form), and for Na (individual form I and universal form U).

As a striking example of the quality of the agreement with experiment, we point out the bulk moduli of the polyvalents, which are overestimated by the stabilized jellium model. As shown by Ashcroft and Langreth,[25] band-structure effects play a decisive role for the compression properties of the polyvalents. As far as the B' are concerned, the stabilized jellium model gives an approximately universal value ($B' = 3.2$), while the evanescent core potential yields higher values, in closer agreement with the empirical data.

Table IV compares structural energy differences calculated from our local pseudopotential and those from a nonlocal one, also evaluated in second-order perturbation theory.[42–45] (Nonperturbative results[46,47] are also available.) For the "local pseudopotential metals" Al, Mg, and Na, the agreement is excellent. In most cases, the observed ground-state structure is predicted; Ca, Sr, and Ba, for which *sd* hybridization is important, are the only glaring exceptions. Table V shows the convergence of various properties with respect to shells of reciprocal lattice vectors; this convergence is rapid only for the monovalent metals.

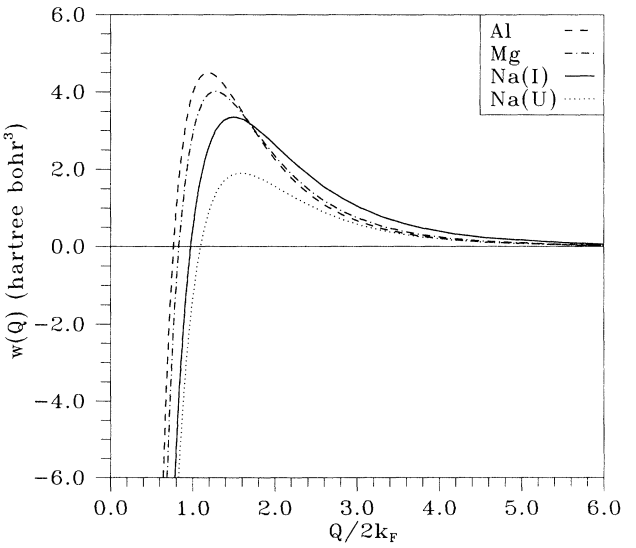

FIG. 2. Evanescent core potential in momentum space for Al and Mg (individual form), and for Na (individual form I and universal form U).

TABLE IV. Energy differences per valence electron (Δe) between different crystal structures, in meV, as calculated from the individual pseudopotential (I) and from a nonlocal pseudopotential (GPT, Refs. 42–44), both treated in second-order perturbation theory. GPT values in parentheses include *sd* hybridization. X labels the nominally exact ground-state structure. Calculated values for a given metal assume the same r_s for each crystal structure. The hcp structures we have considered for the non-hcp metals are ideal, with $c/a = 1.633$. Although Li and Na are conventionally bcc, the hcp structure is really lower in energy (Ref. 62). Under pressure, Pb makes a phase transition to an unknown structure, usually considered to be hcp, while Tl changes over to fcc (Ref. 63).

Metal	Structure		fcc-bcc		fcc-hcp		bcc-hcp	
	I	X	I	GPT	I	GPT	I	GPT
Be	hcp	hcp	-15.2		1.1		16.2	
Al	fcc	fcc	-28.6	-33.1	-7.4	-7.7	21.2	25.4
Pb	hcp	fcc	-1.3		1.6		2.8	
Tl	hcp	hcp	-3.8		0.4		4.3	
Mg	hcp	hcp	-9.2	-9.5	4.0	4.1	13.2	13.6
Li	hcp	hcp	-0.4		0.0		0.4	
Ca	hcp	fcc	-5.2	-2.3	5.8	2.1	11.0	4.4
				(-8.8)		(-5.4)		(3.4)
Sr	hcp	fcc	-4.5	(-12.2)	5.5	(-3.4)	10.0	(8.8)
Ba	hcp	bcc	-4.8		4.6		9.3	
Na	hcp	hcp	-0.4	-0.7	0.1	0.2	0.5	0.9
K	bcc	bcc	0.1		0.0		-0.1	
Rb	bcc	bcc	0.1		0.0		-0.0	
Cs	bcc	bcc	0.1		0.0		-0.1	

IV. CONCLUSIONS

The controlling properties of an *sp*-bonded metal are the equilibrium average valence electron density parameter r_s and valence z. Together they define the Wigner-Seitz radius r_0, which is set in part by the decay length $R_{\rm HF}$ of the highest-energy s or p core orbital of the free atom:

$$r_0 \equiv z^{\frac{1}{3}} r_s \approx 7 R_{\rm HF} \tag{4.1}$$

from Table II. A third controlling solid-state property is the interstitial electron density[2,3,48] (or, alternatively, the first zero of the form factor).

A useful zero-order picture of a simple metal is the stabilized jellium or structureless pseudopotential model,[5]

TABLE V. Partial sums of properties over the first n shells of reciprocal lattice vectors. $n = 0$ corresponds to $G = 0$, $n = 1$ includes also the shortest nonzero reciprocal lattice vectors with nonzero structure factors, etc. The number of reciprocal lattice vectors included in a calculation is roughly $4zx^3$, where $x = 0.44\, G_{\max}(n)/2k_F + 0.56\, G_{\max}(n+1)/2k_F$ and z is the valence. (Individual or "I" pseudopotentials.) Note that the structural energy differences for Al, Mg, and Na (Table IV) are converged for $G_{\max}/2k_F \geq 4$.

Metal	Property	$n=0$	$n=1$	$n=2$	$n=3$	$n=4$	$n=5$	$n=\infty$
Al	$G_{\max}/2k_F$	0	0.768	0.887	1.255	1.471	1.537	
(fcc)	e (eV)	-18.19	-18.19	-18.30	-18.53	-18.78	-18.85	-19.05
	P (Mbar)	0.24	0.25	0.10	0.03	-0.01	-0.02	0.00
	B (Mbar)	2.054	1.271	0.764	0.702	0.714	0.721	0.771
	B'	2.94	3.10	4.05	4.53	4.64	4.65	4.39
	μ (eV)	0.70	0.70	0.64	0.37	0.10	0.03	-0.17
	N_{int}	0.779	0.776	0.782	0.709	0.686	0.686	0.705
Mg	$G_{\max}/2k_F$	0	0.828	0.882	0.938	1.210	1.434	
(hcp)	e (eV)	-11.71	-11.71	-11.71	-11.79	-11.83	-11.88	-12.12
	P (Mbar)	0.09	0.09	0.08	0.02	0.01	4×10^{-3}	0.00
	B (Mbar)	0.660	0.614	0.552	0.313	0.299	0.297	0.314
	B'	2.91	2.92	3.02	4.01	4.19	4.27	4.17
	μ (eV)	-0.81	-0.81	-0.82	-0.88	-0.92	-0.98	-1.23
	N_{int}	0.526	0.524	0.533	0.574	0.560	0.542	0.529
Na	$G_{\max}/2k_F$	0	1.140	1.612	1.974	2.280	2.549	
(bcc)	e (eV)	-6.08	-6.13	-6.16	-6.20	-6.21	-6.22	-6.23
	P (Mbar)	0.01	8×10^{-4}	-1×10^{-4}	-6×10^{-4}	-6×10^{-4}	-4×10^{-4}	0.00
	B (Mbar)	0.097	0.069	0.069	0.070	0.070	0.070	0.071
	B'	2.97	3.60	3.68	3.67	3.65	3.63	3.62
	μ (eV)	-1.83	-1.90	-1.93	-1.97	-1.98	-1.99	-2.00
	N_{int}	0.320	0.358	0.350	0.338	0.338	0.340	0.341

which requires as inputs only r_s and z. But this model overestimates the bulk modulus B and underestimates its pressure derivative B' for the polyvalents. These defects can be repaired with the help of a structured pseudopotential.

We have proposed a local pseudopotential $w(r)$ with an exponentially decaying repulsion from the core at large r and simple analyticity conditions at small r. Two versions of the pseudopotential have been considered, with universal and individual choices for the parameters. Both versions are designed to give bulk stability at the observed density. A second-order perturbative calculation with these pseudopotentials has shown good agreement of predicted physical properties (e, B, and B') with experiment. The individual pseudopotential, which reproduces the correct equilibrium interstitial electron density for each metal, has been found to be generally the better choice. Moreover, the exponential decay length of the core repulsion matches that of the highest-energy s or p core orbital, corroborating the physical picture from which the potential was constructed, and the value Q_0 of the first zero of the form factor agrees with conventional values. For Al, Mg, and Na, our structural energy differences are very close to those of a good nonlocal pseudopotential.

Bulk moduli are predicted more accurately by this local pseudopotential than by first-principles nonlocal norm-conserving ones. Of course, nonlocal pseudopotentials fitted to *solid-state* inputs (including r_s, z, and the interstitial density) would be potentially more accurate and more transferable than any local forms. To incorporate nonlocality, the evanescent core form (2.3) could be applied separately to each angular-momentum component of the Bloch orbitals; to improve transferability, nonlinear core contributions[49] to the exchange-correlation potential could be invoked. Nevertheless, we stress the convenience and physical transparency of local pseudopotentials, and the need for them in quantum Monte Carlo tests[12,13] of density functional approximations.

From previous work,[50–52] it appears that a pseudopotential constructed from a first-order description of the electron density or a second-order description of the energy is appropriate for a calculation of metallic properties in the same order of perturbation theory. This justifies our use of low-order perturbation theory. If, however, a nonperturbative method is to be used, the pseudopotential parameters should in principle be reoptimized for that choice. In view of the remarkable accuracy of second-order pseudopotential perturbation theory for the total energy of a close-packed perfect crystal,[39] we would not expect much change in these parameters. (For the individual pseudopotential description of the metals in Table III, $0.05 \leq |e_{\text{BS}}|/e_F \leq 0.10$, where $e_F = k_F^2/2$.)

Possible further applications of our local pseudopotential include the Fermi surface, bulk and surface phonon frequencies, Car-Parrinello dynamics, atomistic description of surfaces, clusters, vacancies and alloys, generalization to semiconductors, etc. While elements like silicon[53] or carbon do not crystallize in close-packed structures, such structures may still be posited for the sake of pseudopotential construction. Alternatively, the pseudopo-

tential could be chosen to reproduce the bond-center density[54] of the observed open structure. Even transition elements may be described by a local pseudopotential, provided that the valence is chosen large enough.[31]

The empirical input to our pseudopotential, r_s, could easily be replaced by the r_s output from an all-electron solid-state calculation, at a slight cost in accuracy. To construct our pseudopotential, we have also employed the observed crystal structure, which could be replaced by the prediction of an all-electron calculation, or by any close-packed structure, with little effect. In any case, it is clear that the inputs r_s and z set mainly the $Q \to 0$ limit of the repulsive part of the pseudopotential $w(Q)$, while the input interstitial density sets $w(Q)$ only for Q equal to nonzero reciprocal lattice vectors, and mainly for the shortest ones.

ACKNOWLEDGMENTS

This work was supported by NATO Collaborative Research Grant No. 910623. The work of J.P.P., J.M.M., and S.Q.A. was also supported by the U.S. National Science Foundation under Grant No. DMR92-13755. J.M.M. was supported in part by AKZO Corporate America, LEQSF (1993-95)-RD-B-15, and DOE/LEQSF (1993-95)-03.

[1] P. Hohenberg and W. Kohn, Phys. Rev. **136**, B864 (1964).
[2] V. L. Moruzzi, J. F. Janak, and A. R. Williams, *Calculated Electronic Properties of Metals* (Pergamon, New York, 1978).
[3] J. H. Rose and H. B. Shore, Phys. Rev. B **49**, 11 588 (1994); **48**, 18 254 (1993).
[4] A. R. Miedema, R. Boom, and F. R. de Boer, J. Less-Common Met. **41**, 283 (1975); R. Boom, F. R. de Boer, and A. R. Miedema, *ibid.* **45**, 237 (1978).
[5] J. P. Perdew, H. Q. Tran, and E. D. Smith, Phys. Rev. B **42**, 11 627 (1990); C. Fiolhais and J. P. Perdew, *ibid.* **45**, 6207 (1992); M. Brajczewska, C. Fiolhais, and J. P. Perdew, Int. J. Quantum Chem. **S27**, 249 (1993); J. P. Perdew, M. Brajczewska, and C. Fiolhais, Solid State Commun. **88**, 795 (1993).
[6] W. A. Harrison, *Pseudopotentials in the Theory of Metals* (W. A. Benjamin, New York, 1966).
[7] M. L. Cohen and V. Heine, in *Solid State Physics: Advances in Research and Applications*, edited by F. Seitz, D. Turnbull, and H. Ehrenreich (Academic, New York, 1970), Vol. 24, p. 37.
[8] W. E. Pickett, Comput. Phys. Rep. **9**, 117 (1989); L. Szasz, *Pseudopotential Theory of Atoms and Molecules* (Academic, New York, 1989).
[9] R. M. Dreizler and E. K. U. Gross, *Density Functional Theory* (Springer, Berlin, 1990).
[10] B. J. Austin, V. Heine, and L. J. Sham, Phys. Rev. **127**, 276 (1968).
[11] G. B. Bachelet, D. R. Hamann, and M. Schlüter, Phys. Rev. B **26**, 4199 (1982).
[12] L. Mitás and R. M. Martin, Phys. Rev. Lett. **72**, 2438 (1994).
[13] H.-J. Flad, A. Savin, M. Schultheiss, A. Nicklass, and H. Preuss, Chem. Phys. Lett. **222**, 274 (1994); H.-J. Flad, A. Savin, and H. Preuss, J. Chem. Phys. **97**, 459 (1992).
[14] I. J. Robertson, V. Heine, and M. C. Payne, Phys. Rev. Lett. **70**, 1944 (1993); I. J. Robertson, D. I. Thomson, V. Heine, and M. C. Payne, J. Phys. Condens. Matter **6**, 9963 (1994).
[15] W. Kohn and L. J. Sham, Phys. Rev. **140**, A1133 (1965).
[16] T. L. Gilbert, Phys. Rev. B **12**, 2111 (1975).
[17] M. Y. Chou, P. K. Lam, and M. L. Cohen, Phys. Rev. B **28**, 4179 (1983).
[18] P. K. Lam and M. L. Cohen, Phys. Rev. B **24**, 4224 (1981).
[19] Y.-M. Juan and E. Kaxiras, Phys. Rev. B **48**, 14 944 (1993).
[20] M. M. Dacorogna and M. L. Cohen, Phys. Rev. B **34**, 4996 (1986).
[21] W. Maysenhölder, S. G. Louie, and M. L. Cohen, Phys. Rev. B **31**, 1817 (1985).
[22] C. Fiolhais, F. Nogueira, and J. P. Perdew, Bull. Am. Phys. Soc. **40**, 252 (1995).
[23] C. Fiolhais, M. Brajczewska, J. P. Perdew, and S. Q. Armster, in *Many-Body Physics*, edited by C. Fiolhais, M. Fiolhais, C. Sousa, and J. N. Urbano (World Scientific, Singapore, 1994).
[24] M. Hasegawa and W. H. Young, J. Phys. F **11**, 977 (1981).
[25] N. W. Ashcroft and D. C. Langreth, Phys. Rev. **155**, 682 (1967).
[26] V. Heine and I. Abarenkov, Philos. Mag. **9**, 451 (1964); I. Abarenkov and V. Heine, *ibid.* **12**, 529 (1965); A. O. E. Animalu and V. Heine, *ibid.* **12**, 1249 (1965).
[27] R. W. Shaw, Phys. Rev. **174**, 769 (1968).
[28] D. D. Ling and C. D. Gelatt, Phys. Rev. B **22**, 557 (1980).
[29] H. Hellmann, Acta Physicochim. URSS **1**, 913 (1934); J Chem. Phys. **3**, 61 (1935).
[30] J. Callaway and P. Laghos, Phys. Rev. **187**, 192 (1969).
[31] T. Starkloff and J. D. Joannopoulos, Phys. Rev. B **16**, 5212 (1977); D. Vanderbilt and J. D. Joannopoulos, *ibid.* **27**, 6296 (1983).
[32] G. L. Krasko and Z. A. Gurskii, Fiz. Tverd. Tela (Leningrad) **13**, 2463 (1971) [Sov. Phys. Solid State **13**, 2062 (1972)].
[33] J. P. Perdew and Y. Wang, Phys. Rev. B **45**, 13 244 (1992).
[34] G. W. Fernando, J. W. Davenport, R. E. Watson, and M. Weinert, Phys. Rev. B **40**, 2757 (1989).
[35] D. D. Koelling and B. N. Harmon, J. Phys. C **10**, 3107 (1977).
[36] H. J. Monkhorst and J. D. Pack, Phys. Rev. **13**, 5188 (1976).
[37] J. Hafner, *From Hamiltonians to Phase Diagrams* (Springer, Berlin, 1986).
[38] J. P. Perdew and T. Datta, Phys. Status Solidi B **102**, 283 (1980).
[39] V. Heine and D. Weaire, Solid State Phys. **24**, 249 (1980).
[40] C. F. Fischer, *The Hartree-Fock Method for Atoms* (J. Wiley, New York, 1977).
[41] J. P. Desclaux, At. Data Nucl. Data Tables **12**, 311 (1973).
[42] A. K. McMahan and J. A. Moriarty, Phys. Rev. B **27**, 3235 (1983).
[43] J. A. Moriarty, Phys. Rev. B **16**, 2537 (1977).

[44] J. A. Moriarty, Phys. Rev. B **34**, 6738 (1986).
[45] J. D. Althoff, P. B. Allen, R. M. Wentzcovitch, and J. A. Moriarty, Phys. Rev. B **48**, 13 253 (1993).
[46] P. K. Lam and M. L. Cohen, Phys. Rev. B **27**, 5986 (1983).
[47] R. M. Wentzcovitch and M. L. Cohen, Phys. Rev. B **37**, 5571 (1988).
[48] J. R. Chelikowsky, Phys. Rev. B **21**, 3074 (1980); J. A. Alonso, D. J. González, and M. P. Iñiguez, J. Phys. F **10**, 1995 (1980).
[49] S. G. Louie, S. Froyen, and M. L. Cohen, Phys. Rev. B **26**, 1738 (1982).
[50] M. Rasolt, J. Phys. C **5**, 2333 (1972).
[51] L. Dagens, M. Rasolt, and R. Taylor, Phys. Rev. B **11**, 2726 (1975).
[52] J. P. Perdew and S. H. Vosko, J. Phys. F **6**, 1421 (1976).
[53] J. Harris and R. O. Jones, Phys. Rev. Lett. **41**, 191 (1978).
[54] N. H. March, Int. J. Quantum Chem. **52**, 247 (1994).
[55] J. Emsley, *The Elements* (Clarendon, Oxford, 1991).
[56] J. H. Rose, J. R. Smith, F. Guinea, and J. Ferrante, Phys. Rev. B **29**, 2963 (1984).
[57] D. J. Steinberg, J. Phys. Chem. Solids **43**, 1173 (1982).
[58] K. Takemura, Phys. Rev. B **44**, 545 (1991).
[59] T. Kenichi, Phys. Rev. B **50**, 16 238 (1994).
[60] M. S. Anderson and C. A. Swenson, Phys. Rev. B **28**, 5395 (1983).
[61] V. Heine and C. H. Hodges, J. Phys. C **5**, 225 (1972); C. H. Hodges, J. Phys. F **4**, 1961 (1974). The argument of Hodges correctly predicts that the stabilized jellium chemical potential $\mu^{\mathrm{SJ}}(z,\overline{n})$ in our Table III equals $e^J(\overline{n})$ of Eq. (3.1). Coupled to the Thomas-Fermi approximation, it further predicts that the universal pseudopotential chemical potential $\mu^U(z,\overline{n})$ should also equal $e^J(\overline{n})$, a relationship only roughly obeyed in Table III.
[62] W. B. Pearson, *Handbook of Lattice Spacing and Structures of Metals and Alloys* (Pergamon, London, 1958); Vol. II (Pergamon, London, 1967).
[63] W. Klement, Jr. and A. Jayaraman, Prog. Solid State Chem. **3**, 289 (1966).